

Influence of plasma induced by radionuclide layer on the radar cross section of spherical objects*

LIU Wei (刘伟), ZHU Jia-Zhu (朱家柱), CUI Chi (崔驰), WANG Xiang (王翔), ZHANG Shi-Yuan (张世远), ZHANG Rui-Li (张瑞利), TANG Tao (唐涛), and HUANG Run-Sheng (黄润生)[†]
School of Physics, Nanjing University, Nanjing 210093, China

(Received December 5, 2014; accepted in revised form January 22, 2015; published online August 20, 2015)

The influence of the α -decay radionuclide layer (the energy of α -particles are 5.45 MeV) on the radar cross section (RCS) of sphere objects was calculated under different radioactivities, frequencies, and sphere radii. When the sphere radius is smaller than 50 cm, the tendency of the electron densities of the plasma slab is to ascend first and then descend, and the typical maximum electron densities with a radioactivity of 10 Ci/cm² raises from 7.02×10^{10} to 1.76×10^{11} when the sphere radii increases from 10 to 300 cm. The average data of a normalized RCS of a sphere with radius of 12.5 cm, which is coated with a radionuclide layer with different radioactivities are -0.35, -0.50, -0.79 and -1.13 dB when the radioactivity is 1, 2, 5 and 10 Ci/cm², respectively.

Keywords: Electromagnetic radiation; Plasma; α -particles; Radar cross section; Sphere object

DOI: [10.13538/j.1001-8042/nst.26.040502](https://doi.org/10.13538/j.1001-8042/nst.26.040502)

I. INTRODUCTION

In the recent years, the plasma stealth technique has gotten more and more attentions because of its smaller impact on the shape of objects and better suitability in a wide frequency band [1–3]. Many techniques can produce plasma: arc discharge, laser excitation, electron guns, or radioactive isotopes [4–7]. When the frequencies of plasma generated from the radioactive isotopes commensurate with the frequencies of electromagnetic waves (EMWs), the damping loss resulting from the excitation in the plasma slab by EMW reaches the maximum. Therefore, the plasma stealth technique by radioactive isotopes is superior, especially in the ultra high frequency (UHF) and super high frequency (SHF) bands.

Sphere metal objects are the most useful in the calibration body of the radar cross section (RCS) field [8, 9]. In past years, many teams had worked out the influence of RCS on different plasma densities and shapes, but most of their research was under their own definition of density or shape [10–17]. These works could be considered a verification of plasma theory, but for actual application, there is still a pronounced gap. This paper aims to calculate the influence of plasma induced by a radionuclide layer (RNL), which is coated on the surface of a sphere metal object, on the RCS in different radioactivities and ratios of the radii of the sphere to the electromagnetic wavelength (RRW).

II. THEORETICAL PRINCIPLE AND RESEARCH METHODS

A. Model

Figure 1 is a schematic drawing of the simulation. A thin RNL is coated on the surface of the spherical metal object. The common radioactive isotopes of α -decay are Po-210 (5.304 MeV, 138.4d), Pu-238 (5.456 and 5.499 MeV, 87.7a) and Am-241 (5.443 and 5.485 MeV, 432.6a). The energy of the α -particles ejected from all the three isotopes are similar, meaning the energy loss of a distance unit of these α -particles is also similar. In our paper, all the calculations are under the α -particle energy of 5.45 MeV as the representative, which possesses no obvious differences of energy loss in air with the three aforementioned isotopes. We assume the material of the spherical metal object is the perfect electric conductor (PEC) because the surface effect depths of most metals are much less than the regular radius of the sphere object. When the EMW propagates into the plasma slab referable to the ionization effect of α -particles, the damping loss of charged particles would decrease the energy of the EMW, and it also would refract the spatial distribution of EMW. All these will influence the RCS of the spherical metal objects.

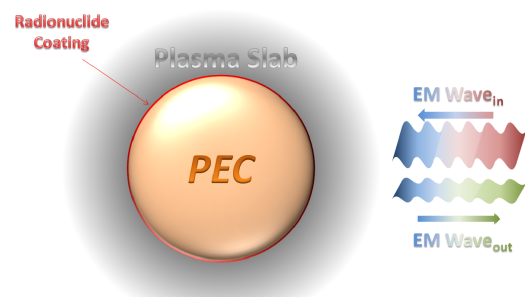


Fig. 1. (Color online) The schematic drawing of the simulation.

* Supported by National Natural Science Foundation of China (Nos. 50977042 and 10904061) and the program of Ministry of Science and Technology of China (No. 2006AA03Z458)

[†] Corresponding author, ruhuang@nju.edu.cn

B. Electron density distribution in plasma slab induced by α -particles

As the velocity of α -particles is much less than light, we can get the average number of new-born ions and ionization electrons by a single α -particle using the nonrelativistic Bethe-Bloch formula and an average ionization energy of 36.08 eV in air [18]

$$\left(\frac{-dE}{dx}\right)_{\text{ion}} \approx \frac{4\pi z^2 e^4 N Z}{(m_0 v^2)} \ln\left(\frac{2m_0 v^2}{I}\right). \quad (1)$$

The frequency of plasma is mainly determined by the density of electrons, because the mass of the electron is much less than the ion. In the simulation, we could only trace these ionization electrons, as a result. In the air, the new-born ionization electrons mainly have three physical processes: diffusion, recombination with positive ions, and adsorption by neutral molecules. During these processes, the negative oxygen ions formed by adsorption dissociate rapidly under ultraviolet rays when the ionized electrons reach a specific energy [19]. In our calculation, we neglected the adsorption process and the elimination would not bring any substantive effects to the results.

The diffusion velocity of electrons is related to the gradient of the electron density (n_e), and considering the effect of ambipolar diffusion in the plasma slab, the coefficient of diffusion is $D_{\text{dif}} = 3.7 \times 10^2 \text{ cm}^2/\text{s}$.

$$\left(\frac{dN}{dt}\right)_d = D_{\text{dif}} \nabla n_e. \quad (2)$$

The recombination velocity is proportional to the concentrations of both positive and negative ions. The whole plasma slab system is close to neutral, so we could consider that the numbers of positive ions and electrons are nearly the same, and the coefficient of recombination is $\alpha = 1.5 \times 10^{-6} \text{ cm}^3/\text{s}$ (both the coefficients are validated by experiments).

$$\left(\frac{dn_e}{dt}\right)_r = \alpha n^+ n_e \approx \alpha n_e^2. \quad (3)$$

The final density of electrons is determined by diffusion, recombination, and ionization by α -particles. Figure 2 is the flow chart of the simulation. The time gap of each cycle is the average time gap between the adjacent two ejected α -particles in one square centimeter, which is determined by the radioactivity of the RNL.

C. The interaction between EMW and plasma

In the plasma slab, there exist four kinds of collisions between electrons and molecules, electrons and ions, ions and molecules, and electrons and electrons. The collisions mostly happen between electrons and molecules in the troposphere. Ginzburg defined a coefficient named effective collision frequency [20], when the frequency of EMW is much smaller

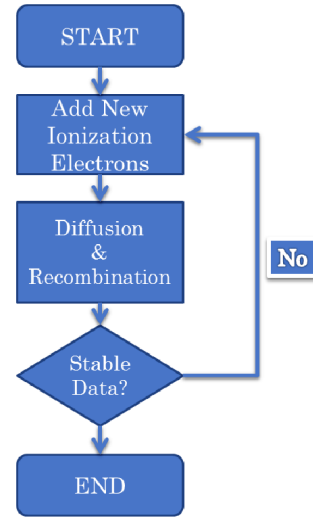


Fig. 2. (Color online) The flow chart of the simulation of electron density.

than the effective collision frequency, the latter could be formulated as

$$\nu \sim \nu_{\text{eff},l} \approx 1.5 \times 10^{11} \frac{N_m}{2.7 \times 10^{19}} \sqrt{\frac{T}{300}}, \quad (4)$$

where N_m is the number of molecules per unit of volume.

But the effective collision frequency exhibits an impact on the EMW frequency. The relationship with the relative dielectric constant and effective collision frequency is

$$\varepsilon_r = 1 - K_1 \frac{\omega_{pe}^2}{\omega_0^2 + \nu_{\text{eff},l}^2} - jK_2 \frac{\nu}{\omega_0} \frac{\omega_{pe}^2}{\omega_0^2 + \nu_{\text{eff},l}^2}, \quad (5)$$

where K_1 and K_2 are two coefficients related to ratio of EMW frequency to the effective collision frequency [20], and

$$\omega_p \approx \omega_{pe} = \sqrt{\frac{n_e e^2}{m_e \varepsilon_0}}. \quad (6)$$

The plasma slab induced by the RNL, which is coated on the surface of the spherical object, is isotropic, that means the density distribution is only related to the radial distance, r . So the plasma slab could be divided into m layers and the radius of the boundary between the $i-1$ th and i th layer is set as a_i : when $0 \leq r \leq a_1$, the material is a perfect electric conductor (PEC); the relative dielectric constant of the i th layer is $\varepsilon_{r,i}$ and the relative permeability is 1, approximately. The relationship between the RCS and scattering coefficients b_n and c_n is

$$\sigma = \frac{c^2}{\pi f^2} (|A_c|^2 \cos^2 \varphi + |A_s|^2 \sin^2 \varphi), \quad (7)$$

and

$$|A_c|^2 = \left| \sum_{n=0}^{\infty} j^n \left[b_n \sin \theta P_n^{1'}(\cos \theta) - c_n \frac{P_n^1(\cos \theta)}{\sin \theta} \right] \right|^2,$$

$$|A_s|^2 = \left| \sum_{n=0}^{\infty} j^n \left[b_n \frac{P_n^1(\cos \theta)}{\sin \theta} - c_n \sin \theta P_n^{1'}(\cos \theta) \right] \right|^2. \quad (8)$$

The scattering coefficients b_n and c_n are calculated by

$$b_n = -\frac{\hat{J}_n'(k_0 a_m) - R_{b,m} \hat{J}_n(k_0 a_m)}{\hat{H}_n^{(2)'}(k_0 a_m) - R_{b,m} \hat{H}_n^{(2)}(k_0 a_m)} a_n,$$

$$c_n = -\frac{\hat{J}_n(k_0 a_m) - R_{c,m} \hat{J}_n'(k_0 a_m)}{\hat{H}_n^{(2)}(k_0 a_m) - R_{c,m} \hat{H}_n^{(2)'}(k_0 a_m)} a_n, \quad (9)$$

in which

$$a_n = j^{-n} \frac{2n+1}{n(n+1)}. \quad (10)$$

And the recurrent relationship of the coefficient $R_{b,m}$ and $R_{c,m}$

$$R_{b,i} = \sqrt{\frac{\varepsilon_{r,i+1}}{\varepsilon_{r,i}}} \frac{\hat{J}_n'(k_i a_i) + \chi_{b,i} \hat{Y}_n'(k_i a_i)}{\hat{J}_n(k_i a_i) + \chi_{b,i} \hat{Y}_n(k_i a_i)},$$

$$R_{c,i} = \sqrt{\frac{\varepsilon_{r,i+1}}{\varepsilon_{r,i}}} \frac{\hat{J}_n(k_i a_i) + \chi_{c,i} \hat{Y}_n(k_i a_i)}{\hat{J}_n'(k_i a_i) + \chi_{c,i} \hat{Y}_n'(k_i a_i)}, \quad (11)$$

$$\chi_{b,i+1} = -\frac{\hat{J}_n'(k_{i+1} a_i) - R_{b,i} \hat{J}_n(k_{i+1} a_i)}{\hat{Y}_n'(k_{i+1} a_i) - R_{b,i} \hat{Y}_n(k_{i+1} a_i)},$$

$$\chi_{c,i+1} = -\frac{\hat{J}_n(k_{i+1} a_i) - R_{c,i} \hat{J}_n'(k_{i+1} a_i)}{\hat{Y}_n(k_{i+1} a_i) - R_{c,i} \hat{Y}_n'(k_{i+1} a_i)}. \quad (12)$$

Because the material of the sphere core is PEC,

$$\chi_{b,2} = -\frac{\hat{J}_n'(k_2 a_1)}{\hat{Y}_n'(k_2 a_1)},$$

$$\chi_{c,2} = -\frac{\hat{J}_n(k_2 a_1)}{\hat{Y}_n(k_2 a_1)}. \quad (13)$$

And the monostatic RCS is one of the particular cases ($\theta = \pi$), so the RCS could be simplified as

$$\sigma = \frac{c^2}{\pi f^2} \left| \sum_{n=1}^{\infty} \frac{1}{2} (-j)^n n(n+1) (b_n - c_n) \right|^2. \quad (14)$$

All the RCS values are represented in the normalized results, $10 \lg \frac{\sigma}{\pi r^2}$, in which r is the radius of the spherical object.

III. RESULTS AND DISCUSSION

A. Electron density distribution in plasma slab

The average range of 5.45 MeV α -particles is 3.84 cm in the air at normal pressure and temperature; the track of a single α -particle is almost straight along the ejection direction. By the simulated average energy loss along the radial direction in consideration of the surface curvature of the spherical metal objects and the randomness of ejection direction, we can get the average electron density per unit volume ionized by a single α -particle, shown in Fig. 3. The solid angle per square centimeter on the surface increases with the decrease of sphere radius, so the average electron densities ionized by a single α -particle decrease. When the sphere radius is smaller than 50 cm, the results show that the tendency of electron densities is to ascend first and then descend. It could be attributed to the effect of the sphere curvature for a relatively small radius, which would cause the decrease of the effective RNL surface with distance, in the proximal region to the surface. Under the combined interaction of the effective RNL surface and the volume corresponding to a unit of solid angle, the radial electron densities possess tendency phenomena with the distance to the sphere.

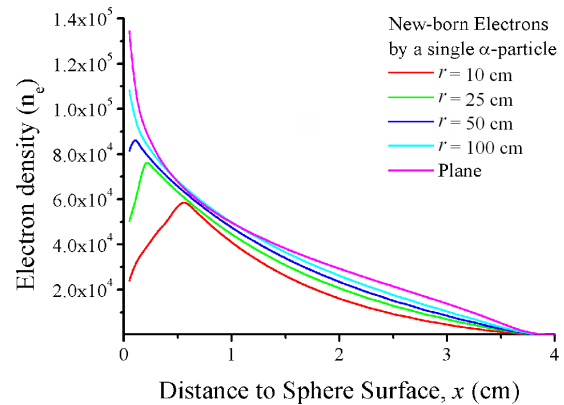


Fig. 3. (Color online) The average radial electron density by a single α -particle per square centimeter.

Based on the average radial electron density and flow chart shown in Fig. 2, we have calculated the actual electron density at different radii and radioactivities. In the calculation, we set the thickness of the plasma slab at 50 cm, which is much larger than the range of α -particle. The consideration of the diffusion effects and the results are shown in Fig. 4. The electron density increases with the radius when the radioactivity of RNL is $1 \mu\text{Ci}/\text{cm}^2$; the maximum density data are 2.42×10^7 , 3.52×10^7 , 4.48×10^7 and 5.17×10^7 corresponding to the sphere radii of 10, 25, 50 and 100 cm, respectively, and the results are close to a value 5.76×10^7 for an infinite large plate ($r \rightarrow \infty$).

When the radioactivity increases 10 times, the ratios of the electron density data with radioactivity at a certain value to the data with ten times the amount of radioactivity are basically consistent for the same sphere radii. The ratio, ex-

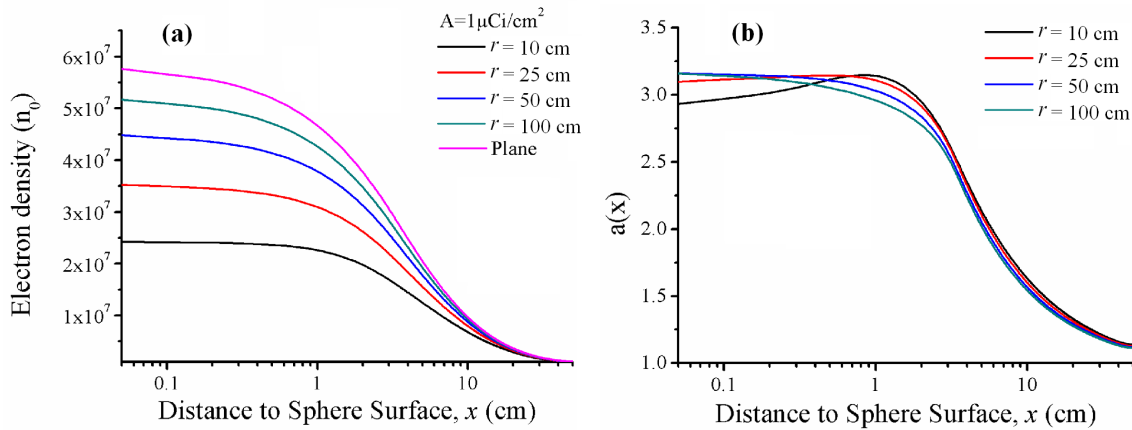


Fig. 4. (Color online) (a) The electron density of $1 \mu\text{Ci}/\text{cm}^2$ with distance to sphere surface at different radii, (b) the activity coefficients at different radii.

pressed as $a(x)$ and denominated by the activity coefficient, is shown in Fig. 4(b) at different sphere radii. Then we summarized an empirical formula to describe the electron density in the plasma slab induced by 5.45 MeV α -particles with the distance to the sphere surface. When the radioactivity is in the range of $1 \mu\text{Ci}/\text{cm}^2$ to $10 \text{ Ci}/\text{cm}^2$, the differences between the empirical equation and the simulation results are less than 3%.

$$n(x) = n_0(x)a(x)^{\lg A}, \quad (15)$$

where $n_0(x)$ represents the electron density data at $1 \mu\text{Ci}/\text{cm}^2$ in Fig. 4(a), x is the distance to sphere surface, A is the surface radioactivity in unit of $\mu\text{Ci}/\text{cm}^2$.

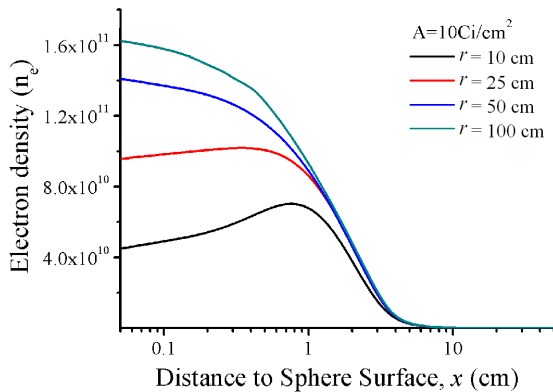


Fig. 5. (Color online) The electron density with x at $10 \mu\text{Ci}/\text{cm}^2$ of radioactivity and different radii by the empirical formula.

In accordance with the empirical formula, we can get the distribution of electron density in conditions of different radii and radioactivities conveniently. Figure 5 is the electron densities with different sphere radii when the radioactivity is $10 \text{ Ci}/\text{cm}^2$ by the empirical formula. When the sphere radii are small, the regions of maximum electron density are not close to the sphere, the tendency of electron density is ascend to first and then descend. For example, when the sphere ra-

dius is 10 cm and the radioactivity of RNL is $10 \text{ Ci}/\text{cm}^2$, the distance between the region of the maximum electron density and the sphere surface is about 1 cm.

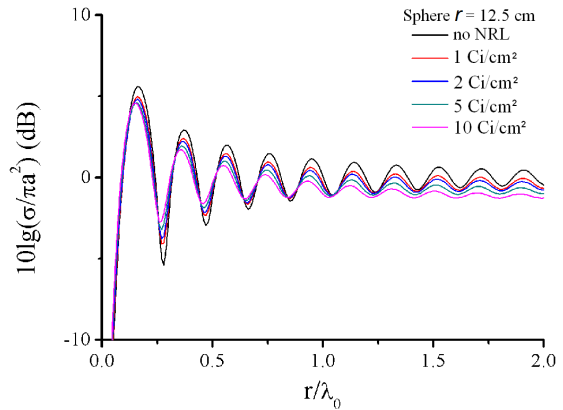


Fig. 6. (Color online) The monostatic RCS at different radioactivities.

B. The influence on monostatic RCS of α -decay RNL

One of the most important parameter is the RRW in the monostatic RCS research on spherical objects. Normally, the normalized RCS data is completely consistent for the same RRWs, due to the relativity of the spatial scale. But the distributions of electron density in the plasma slab outside the spherical object will change with the radii and radioactivity. So in our model, even if the RRWs are the same, there exist differences in the normalized RCS data. Figure 6 is the monostatic RCS data in the radioactivity range from $1 \text{ Ci}/\text{cm}^2$ to $10 \text{ Ci}/\text{cm}^2$ and at a radius of 12.5 cm. The amplitudes of oscillation decrease with the increase of RRW and when $r/\lambda_0 > 1$, the average monostatic RCS data of spherical objects without RNL is 0. The average values decrease with the increase of the radioactivity of RNL: the average data is

−0.35, −0.50, −0.79 and −1.13 dB, respectively, when the radioactivity is 1, 2, 5 and 10 Ci/cm². Also, the amplitudes of oscillation would decrease with the increase of radioactivity, and there exists deviations in the positions of peaks and valleys. The reason is the refraction of incident and scattering waves caused by the inhomogeneous distribution of plasma. The higher electron density indicated by higher radioactivity would result in more obvious refraction.

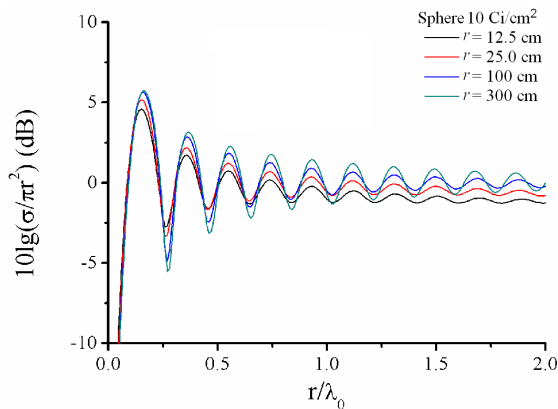


Fig. 7. (Color online) The monostatic RCS at different sphere radii.

Figure 7 shows the monostatic RCS data at different sphere radii and a radioactivity of 10 Ci/cm², and we can also find the differences in these curves with different sphere radii for the same radioactivity. Similarly, the amplitudes of oscillation decrease with the increase of RRW or the decrease of the sphere radius. Certain deviations also exist in the positions of peaks and valleys. The average values of normalized mono-

static RCS when $r/\lambda_0 > 1$ are −1.13, −0.62, −0.26 and −0.09 dB when the sphere radii are 12.5, 25, 100 and 300 cm respectively. The smaller radius means a shorter wavelength for the same RRWs, so the ratio of the thickness of the plasma slab to the EMW wavelength increases with the decrease of the radius. That finally results in more fraction of the EMW with the same RRW when the radius becomes smaller, even though the electron density also becomes smaller under those conditions.

IV. CONCLUSION

The influence of plasma induced by an α -decay RNL on the RCS of spherical metal objects is simulated. First, we calculated the electron density in the plasma slab at different radioactivities and sphere radii. The maximum electron density is about 1.62×10^{11} per cubic centimeter for the RNL radioactivity of 10 Ci/cm² and sphere radius of 1 m. The maximum electron density could increase with the sphere radius for the same radioactivity of RNL. When $r/\lambda_0 > 1$, and the average monostatic RCS data is −0.35, −0.50, −0.79 and −1.13 dB when the radioactivity is 1, 2, 5 and 10 Ci/cm², respectively. Also, when radioactivity is 10 Ci/cm², the average values of normalized monostatic RCS are −1.13, −0.62, −0.26 and −0.09 dB when the sphere radii are 12.5, 25, 100 and 300 cm, respectively. Mostly, the effects on the monostatic RCS increase with the increase of radioactivity or the decrease of the sphere radius for the same RRWs. The simulation results prove that coating RNL can effectively decrease the RCS of spherical object.

- [1] Alexeff I, Kang W L, Rader M, *et al.* A plasma stealth antenna for the US Navy. IEEE International Conference on Plasma Science, 25th Anniversary, 1998, 277–282.
- [2] Petrin A B. On the transmission of microwaves through plasma layer. IEEE T Plasma Sci, 2000, **28**: 1000–1008. DOI: 10.1109/27.887768
- [3] Bliokh Y P, Felsteiner J and Slutsker Y Z. Total absorption of an electromagnetic wave by an overdense plasma. Phys Rev Lett, 2005, **95**: 156003. DOI: 10.1103/PhysRevLett.95.165003
- [4] Li T M, Choi S, Watanabe T, *et al.* Discharge and optical characteristics of long arc plasma of direct current discharge. Thin Solid Films, 2012, **523**: 72–75. DOI: 10.1016/j.tsf.2012.07.061
- [5] Afzal M, Ajmal M, Nusair Khan A, *et al.* Surface modification of air plasma spraying WCC12%Co cermet coating by laser melting technique. Opt Laser Technol, 2014, **56**: 202–206. DOI: 10.1016/j.optlastec.2013.08.017
- [6] Chung K J, Chung K S and Hwang Y S. Dynamics of plasma channel in a parallel-plate plasma gun. Curr Appl Phys, 2014, **14**: 287–293. DOI: 10.1016/j.cap.2013.11.032
- [7] Flierl H P, Engelbrecht M, Engelhardt M P, *et al.* The energy loss of alpha particles traversing a hydrogen plasma. Nucl Instrum Meth A, 1998, **415**: 637–641. DOI: 10.1016/S0168-9002(98)00438-0
- [8] Egel A and Lemmer U. Dipole emission in stratified media with multiple spherical scatterers: Enhanced outcoupling from OLEDs. J Quant Spectrosc Ra, 2014, **148**: 165–176. DOI: 10.1016/j.jqsrt.2014.06.022
- [9] Merchiers O, Moreno F, González F, *et al.* Electromagnetic wave scattering from two interacting small spherical particles. Influence of their optical constants, ϵ and μ . Opt Commun, 2007, **269**: 1–7. DOI: 10.1016/j.optcom.2006.07.040
- [10] Yang H W. Simulation and analysis of interaction between oblique incidence electromagnetic wave and plasma slab. Opt, Int J Light Electron Opt, 2011, **122**: 945–948. DOI: 10.1016/j.ijleo.2010.06.023
- [11] Liu S and Zhong S Y. Analysis of backscattering RCS of targets coated with parabolic distribution and time-varying plasma media. Opt Int J Light Electron Opt, 2013, **124**: 6850–6852. DOI: 10.1016/j.ijleo.2013.05.173
- [12] Daniel J and Tajima T. Electromagnetic waves in a strong Schwarzschild plasma. Phys Rev D, 1997, **55**: 5193–5204. DOI: 10.1103/PhysRevD.55.5193
- [13] Kuehl H H and Zhang C Y. One-dimensional, weakly nonlinear electromagnetic solitary waves in a plasma. Phys Rev E, 1993, **48**: 1316–1323. DOI: 10.1103/PhysRevE.48.1316
- [14] Panchenko A V, Esirkepov T Z, Pirozhkov A S, *et al.* Interaction of electromagnetic waves with caustics in plasma

- flows. Phys Rev E, 2008, **78**: 056402. DOI: [10.1103/PhysRevE.78.056402](https://doi.org/10.1103/PhysRevE.78.056402)
- [15] Kim H C and Verboncoeur J P. Reflection, absorption and transmission of TE electromagnetic waves propagation in a nonuniform plasma slab. Comput Phys Commun, 2007, **17**: 118C121. DOI: [10.1016/j.cpc.2007.02.056](https://doi.org/10.1016/j.cpc.2007.02.056)
- [16] He X, Chen J, Ni X, *et al.* Numerical investigation on interference and absorption of electromagnetic waves in the plasma-covered cavity using FDTD method. IEEE T Plasma Sci, 2012, **40**: 1010–1018. DOI: [10.1109/TPS.2012.2184773](https://doi.org/10.1109/TPS.2012.2184773)
- [17] Ghaffar A, Yaqoob M Z, Alkanhal Majeed A S, *et al.* Scattering of electromagnetic wave from perfect electromagnetic conductor cylinders placed in un-magnetized isotropic plasma medium. Opt, Int J Light Electron Opt, 2014, **125**: 4779–4783. DOI: [10.1016/j.ijleo.2014.04.061](https://doi.org/10.1016/j.ijleo.2014.04.061)
- [18] Wyckof H O. Average energy required to produce an ion pair. ICRU Report. 1979, Washington, DC, USA.
- [19] Zvorykin V D, Ionin A A, Levchenko A O, *et al.* Effects of picosecond terawatt UV laser beam filamentation and a repetitive pulse train on creation of prolonged plasma channels in atmospheric air. Nucl Instrum Meth B, 2013, **309**: 218–222. DOI: [10.1016/j.nimb.2013.02.030](https://doi.org/10.1016/j.nimb.2013.02.030)
- [20] Ginzburg V L. The propagation of electromagnetic waves in plasmas. New York (USA): Pergamon Press, 1970.